SHORT CRACK BEHAVIOUR IN A533B AND En8 STEELS

M. N. James and G. C. Smith

Department of Metallurgy and Materials Science, University of Cambridge, Pembroke Street, Cambridge CB2 3QZ, England

ABSTRACT

Experimental threshold data are reported for small surface cracks in two structural steels. The data show the variation in threshold stress intensity range with stress ratio and crack size. The observed trends are explained in terms of crack closure concepts. In addition, surface crack closure data are presented for a range of stress intensity values.

KEYWORDS

Surface cracks; fatigue; threshold data; crack closure; steels.

INTRODUCTION

When the growth of very small surface cracks (typically under 500 μm deep) is studied it is generally observed that such cracks exhibit lowered thresholds and enhanced growth rates (at low values of ΔK) relative to those obtained with longer cracks. Several possible causes of these enhanced growth rates have been identified:

1) Microstructural effects; i.e. a breakdown in the homogeneous continuum requirement of fracture mechanics, which may occur when cracks are of a similar length to some microstructural dimension (Taylor, 1982).

2) Plasticity effects; i.e. the crack is either growing in a region of bulk plasticity (El Haddad and co-workers, 1980; Dowling, 1977), or is affected by the size of its own crack tip plastic zone and/or microplasticity in favourably orientated grains at the crack tip (Lankford, 1982). Such behaviour may in some cases be normalised by the use of an appropriate fracture mechanics parameter, such as the J integral (Dowling, 1977).

3) Crack closure effects; even when LEFM is applicable to a short crack situation, a breakdown may occur in the assumption that the crack growth rate under a particular loading mode is a unique function of ΔK (McCarver and Ritchie, 1982; James, M.R. and Morris, 1983; James, M.N. and Smith, 1983a). This occurs because parameters like ΔK define the nominal mechanical 'driving force' for crack extension, which is based on the stress and strain fields ahead of the crack tip. They therefore provide little information on

the local effective driving force actually experienced at the crack tip. This effective driving force is likely to be lower than the applied ΔK because of crack closure mechanisms which act in the wake of the crack. Crack closure can be accounted for through the use of the effective stress intensity range ΔK_{eff}, provided that the crack opening load can be determined.

This paper considers the range of crack sizes, in both En8 and A533B steels, which exhibit the enhanced growth rates mentioned above. Crack closure changes are suggested to be the cause of the observed short crack behaviour in the two steels, as crack closure arguments rationalise threshold behaviour, for all crack lengths, over the range of stress ratios considered (0.1 - 0.7).

EXPERIMENTAL PROCEDURE

The materials used were a 0.4% carbon En8 designation steel (BS 970:1955) and a low alloy A533B steel (ASTM specification A533-78). Tables 1 and 2 detail the heat treatments, resultant mechanical strengths and chemical analyses of these steels.

TABLE 1 Heat Treatments and Resultant Tensile Strengths

Steel	Heat Treatment	Lower Yield Strength MPa	UTS MPa
En8	900°C for 1h-WQ 600°C for 1h-WQ	792	891
A533B WQ	900°C for 2h-WQ 600°C for 2h-WQ	799	879
A533B OQ	900°C for 2h-OQ 650°C for 2h-WQ	689	763

WQ = water quenched, OQ = oil quenched

TABLE 2 Chemical Analysis of Major Alloying Elements

Steel	C	Mn	Si	S	P	Ni	Mo
En8	0.40	0.80	0.19	0.041	0.037	-	-
A533B	0.24	1.52	0.25	0.004	0.005	0.62	0.52

(weight per cent)

These heat treatments produced bainitic or martensitic microstructures consisting of finely dispersed carbides in a fine-grained (about 10 μm) ferrite matrix.

All tests were performed in four-point (pure) bend in an air environment and a cyclic testing frequency of 120 - 170 Hz. Crack growth was monitored via cellulose acetate replicas of the surface. The development of crack shape was determined from either light or scanning electron fractographs obtained from post-test fracturing of specimens. The following equation described approximately the development of crack shape in the two steels:

$$a = (0.84c + 20) \quad \mu m$$

for a approximately less than 200 μm, where a is the maximum crack depth and c is half the surface length. As a decreased below 200 μm the aspect ratio remained constant at about 1.07. Thresholds were determined via a stress relief - load incremental technique, details of which are given elsewhere (James and Smith, 1983). The total error in determining values of ΔK_{th} was estimated to be ± 5%. This figure was supported by the experimental results for 'long' cracks, which showed a scatter of about 5% either side of the mean value.

EXPERIMENTAL RESULTS AND DISCUSSION

Figs. 1 and 2 show, for several stress ratios, the experimentally found variation in ΔK_{th} with crack depth for the En8 and A533B respectively.

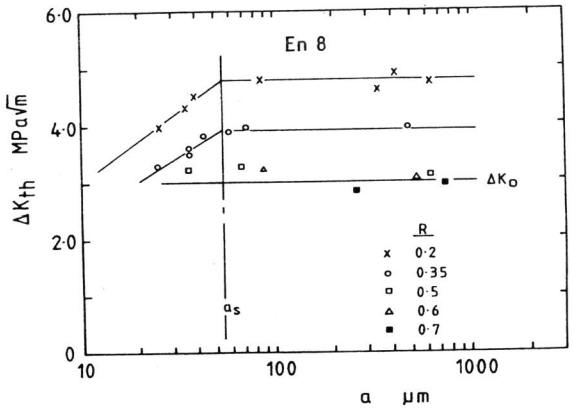

Fig. 1 En8 - variation in ΔK_{th} with crack depth a for several positive stress ratios.

The onset of 'short' crack behaviour, which in these steels results in increased growth rates near the threshold and lowered thresholds relative to longer cracks, is denoted by a_s and occurs at rather small crack depths, i.e. 55 μm for the En8 and about 100 μm for the A533B in both its WQ and OQ conditions. It is clear in Fig. 1 that, for the En8, there is no further decrease in the value of ΔK_{th} for 'long' cracks (i.e. those that can be characterised by a single value of ΔK_{th} irrespective of size) once R > 0.5, and that a crack whose depth is about 35 μm has the same value of ΔK_{th} at R = 0.5, as that found for long cracks (within the bounds of experimental scatter). A similar situation occurs with the A533B results in Fig. 2, with no further decrease in long crack thresholds observed once R > 0.6.

It could be argued that the small size of these short cracks renders the use of LEFM somewhat dubious, for the following reasons:
1) The threshold values of surface stress are quite close to the macroscopic yield stress of the material.
2) The size of the cyclic plastic zone (r_p) at the crack tip is > a/50 (the

ratio a/r_p actually lying in the range 20-30 for the smallest cracks considered here.

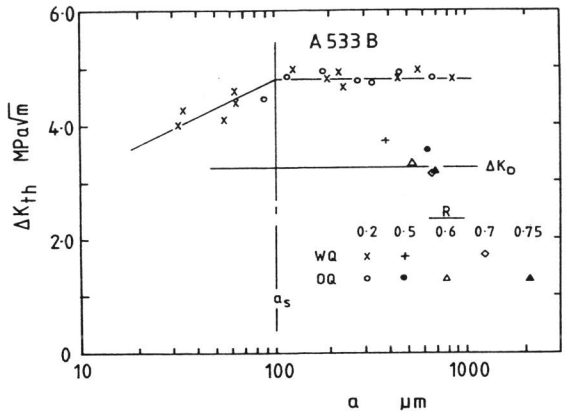

Fig. 2 A533B - variation in ΔK_{th} with crack depth for R = 0.2.

The observed short crack behaviour could then be suggested to be due to the effects of localised plasticity. However, the following points indicate that is not the case for these quenched and tempered steels:

1) Once ΔK is above the knee in the growth rate curve, i.e. in the linear regime of the da/dN - ΔK plot, surface cracks grown in the presence of bulk surface plasticity give data which lie on the same growth rate curve as that obtained from either surface cracks grown under elastic conditions, or long through-cracks. The long through-crack data was acquired using potential drop monitoring of crack length and a compliance function for the ΔK calculations.

2) The data in Fig. 1 for R = 0.5 do not show any evidence of short crack behaviour. If plasticity was the cause of the enhanced growth rates observed with these short cracks, such behaviour should be even more evident at R = 0.5 where the maximum stress at the threshold is becoming high enough to give general surface yielding when the crack size is small.

3) Crack closure measurements were performed on 'long' surface cracks in the En8 steel using a very similar method to that used by Morris (1979), details of these measurements being given elsewhere (James and Smith, 1983b). They indicated that the value of K_{op}/K_{max} (where K_{op} is the stress intensity at which the crack tip is fully open, and K_{max} is the maximum stress intensity in the cycle) in the linear growth rate regime was the same for cracks grown either under elastic conditions or in the presence of surface plasticity. This is demonstrated in Fig. 3, where it can be seen that the value of K_{op}/K_{max} for the crack grown in the presence of bulk plasticity fits the trend line obtained from cracks grown under elastic conditions. It is also clear in Fig. 3 that K_{op}/K_{max} increases as K_{max} decreases, tending to a value of about 0.5 near the threshold for cracks grown at R = 0.1. This increase in K_{op}/K_{max} begins at values of K_{max} around the knee in the da/dN - ΔK curve, i.e. at the transition from the linear regime of growth to near-threshold growth, which for R = 0.1 occurs at approximately K_{max} = 15 MPam$^{\frac{1}{2}}$.

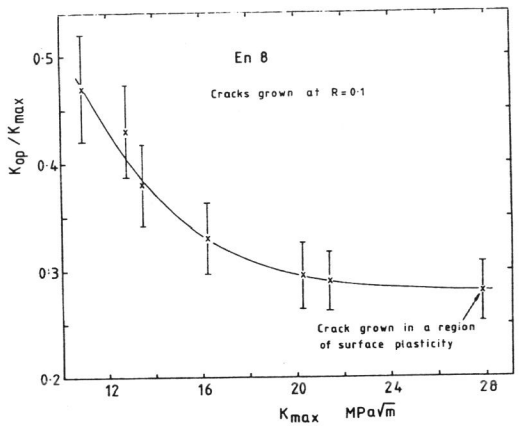

Fig. 3 Results of the crack closure measurements performed on surface microcracks in the En8 steel. a is in the range 166-667 μm.

All the data in Fig. 1 can be normalised into a narrow scatter band around the value of ΔK_o using crack closure concepts, as described in detail elsewhere (James and Smith, 1983a). The approach used in this normalisation is based on the observation that, for both these steels, the effect of stress ratio on the value of ΔK_{th} for long cracks can be explained in terms of the crack closure argument proposed by Schmidt and Paris (1973). This is shown in Fig. 4, which compares the experimentally observed trends in ΔK_{th} with those predicted from crack closure considerations.

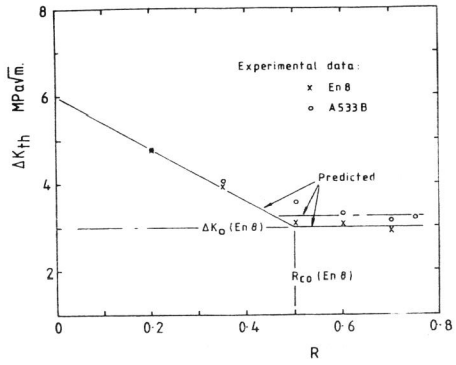

Fig. 4 Comparison of experimental threshold data with the trends predicted using the crack closure argument suggested by Schmidt and Paris.

R_{co} represents the value of stress ratio at which ΔK_{th} first equals the absolute material value of threshold ΔK_o. The original proposal of Schmidt and Paris assumed that K_{op} at the threshold had a constant value, independent of the stress ratio. A requirement of the theory is that $K_{op} = K_{min}$ at the point where $R = R_{co}$, and hence the threshold value of K_{op}/K_{max} (for $R \leq R_{co}$) is then equivalent to the value of R_{co} for the material under consideration. Once ΔK_o and the threshold value of K_{max} at a low stress ratio have been established for a particular material, the predicted lines in Fig. 4 are uniquely defined.

The comparison in Fig. 4 between the experimental data and the predicted linear relationship between ΔK_{th} and R, up to R_{co}, indicates that whilst K_{op}/K_{max} does indeed appear to be constant for the En8, it is not so for the A533B. The two A533B data points at R = 0.35 and 0.5, which are slightly elevated with respect to the theoretical predictions, can be explained in terms of a slight increase in the magnitude of K_{op}/K_{max} as R increases. The value of R_{co} for the En8 (0.5) is in agreement with the data of Fig. 3, which indicates that K_{op}/K_{max} at the threshold value of K_{max} (6 $MPam^{\frac{1}{2}}$ for R = 0 - 0.5) should be about 0.5.

Data in the form presented in Fig. 4 offers the possibility of examining changes in K_{op}/K_{max} for cracks in the short crack regime, through determining the appropriate values of R_{co}. This was done for the En8 steel, giving the results shown in Fig. 5.

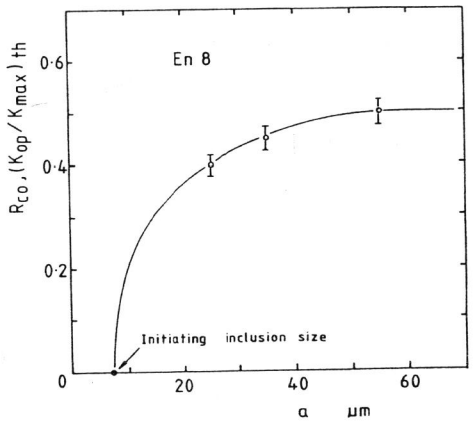

Fig. 5 En8 - change in crack opening level with crack depth in the short crack regime. The data represents the observed variation in R_{co} found with short cracks.

In the limit, it seems reasonable to assume that when a crack is initiated its closure level is approximately zero. This assumption provides the point at which $K_{op}/K_{max} = 0$ (initiating inclusion size is approximately 7 μm). Application of this closure data to the threshold results of Fig. 1 enables all the data to be rationalised into a narrow band of threshold data around the value of ΔK_o obtained for long cracks (James and Smith, 1983a).

Although this is a somewhat circular argument, it does provide an indication that short crack behaviour, in such quenched and tempered steels with fine-scale microstructures, arises from changes in closure level as the crack size becomes very small. In essence, a certain length of crack wake is required to build up a closure level representative of that of long cracks. Crack closure contributions can arise from crack tip plasticity, microstructure (which affects the Mode 11 induced component of closure (Suresh and Ritchie, 1982)) and environment (oxide induced closure (Stewart, 1980)). The interaction of these mechanisms is likely to cause some variation in the extent of the short crack regime from one material to another. This is demonstrated by the difference in a_s for the two steels of the present study, despite the observed similarity of mechanical strengths, threshold stress intensities and microstructure in the En8 and A533B WQ. Fractographic examination of the two steels indicated that fracture surfaces in the A533B were microscopically smoother than those in the En8. In addition, there was more evidence of shear type features at low growth rates in the A533B. It is surmised that these fractographic differences affect the magnitude of the various closure contributions, leading to the different a_s values observed. The actual fracture mechanisms causing these changes in fracture surface topography and the manner in which they affect crack closure are, however, still uncertain.

CONCLUSIONS

1) Short crack behaviour in both En8 and A533B, in the quenched and tempered conditions, appears to be explicable in terms of a breakdown in the fracture mechanics similitude concept. This breakdown is caused by the reduced crack closure level that pertains to short cracks.
2) The extent of the short crack regime is influenced by the applied stress ratio, and short crack behaviour is likely to be absent at high values of stress ratio (R > 0.5 - 0.7).

ACKNOWLEDGEMENTS

The authors would like to thank Professor R. W. K. Honeycombe F.R.S. for the provision of laboratory facilities, and UKAEA Northern Division, Springfields for supplying the A533B steel. One of the authors (MNJ) would also like to thank the Beit Trust for the award of a postgraduate fellowship, and the Committee of Vice-Chancellors and Principals of the Universities of the United Kingdom for the provision of an O.R.S. award.

REFERENCES

Dowling, N. E. (1977). Crack growth during low cycle fatigue of smooth axial specimens. In Cyclic Stress-Strain and Elastic Deformation Aspects of Fatigue Crack Growth, ASTM STP 637, Amer. Soc. Test. Matls., pp. 97-121.

El Haddad, M. H., Dowling, N.E., Topper, T.H. and Smith, K. N. (1980). J integral applications for short fatigue cracks at notches. Int. J. Fract., 16, 15-30.

James, M. N. and Smith, G. C. (1983). Crack closure and surface microcrack thresholds - some experimental observations. Int. J. Fatigue, 5, 75-78.

James, M.N. and Smith, G. C. (1983). Surface microcrack closure in fatigue: a comparison of compliance and crack sectioning data. Int. J. Fract., 22, R69-R75.

James, M. R. and Morris, W. L. (1983). Effect of fracture surface roughness on growth of short fatigue cracks. Metall. Trans., 14A, 153-155.

Lankford, J. (1982). The growth of small fatigue cracks in 7075-T6 aluminium. Fatigue Eng. Mater. Struct., 5, 233-248.

McCarver, J. F. and Ritchie, R. O. (1982). Fatigue crack propagation thresholds for long and short cracks in Rene 95 nickel-base superalloy. Mater. Sci. Eng., 55, 63-67.

Morris, W. L. (1979). Microcrack closure phenomena for Al 2219-T851. Metall. Trans., 10A, 5-11.

Schmidt, R. A. and Paris, P. C. (1973). Threshold for fatigue crack propagation and the effects of load ratio and frequency. In Progress in Flaw Growth and Fracture Toughness Testing, ASTM STP 536, Amer. Soc. Test. Matls., pp. 79-94.

Stewart, A. T. (1980). The influence of environment and stress ratio on fatigue crack growth at near-threshold stress intensities in low-alloy steels. Eng. Fract. Mech., 13, 463-478.

Suresh, S. and Ritchie, R. O. (1982). A geometric model for fatigue crack closure induced by fracture surface roughness. Metall. Trans., 13A, 1637-1631.

Taylor, D. (1982). Fatigue Eng. Mater. Struct., 5, 305-309.